Wavelet Analysis of Business Cycles for validation of Probability of Default:
How does the current credit crunch influences model validation?

Marco van der Burgt[1]

January 2009

Abstract
According to Basel II, the Probability of Default (PD) should be a long-term average of 1-year default rates. In this paper, long term is interpreted as one business cycle. When the PD is compared with the actual observed default rates in the PD rating validation process, two questions are relevant: how long is a business cycle and where are we in the business cycle? We present two techniques in order to address these questions: Fourier analysis and wavelet analysis. The analysis of default rates in the period 1981-2007 from Standard & Poors reveals two business cycles of 10.67 years.

1. Introduction

Under the "International Convergence of Capital Measurement and Capital Standards", hereafter denoted as the Basel II Accord [Basel2004], banks are allowed to develop their own rating models, which is called the Internal Rating Based approach (IRB). A rating assesses the credit quality of an obligor and is therefore mapped to a Probability of Default (PD). According to paragraph 447 of the Basel II Accord, it is required that "PD estimates must be a long-run average of one-year default rates for borrowers in the grade". Although the Basel II Accord does not explicitly define "long term", it is assumed here that this long term refers to the duration of a business cycle.

In this paper, we regard the current credit crisis as part of a business cycle in line with the ideas of Minsky [Minsky1985, Minsky1986, Minsky1993]. Minsky argues that the financial system swings between robustness and fragility, thereby generating business cycles. In his view, a market boom leads to euphoria in which financial institutions extend credit to dubious borrowers, often accompanied by creating new financial instruments and by innovation. As such, the capitalist economy becomes more and more fragile over a period of prosperity. Minsky called this his Financial Instability Hypothesis (FIH).

Minsky's theory, although invented many years ago, exactly matches with the current observation that the current crisis is caused by securitization of mortgages, which enables banks to provide home loans without concern on repayment. Lenders became more creative with exotic mortgages, like "interest only" loans and "option adjustable rate" mortgages, to provide credit to borrowers of poor credit quality. These mortgages were bundled in securitization packages and often sold to unregulated hedge funds by Special Purpose Vehicles. In line with Minsky, the economy destabilizes, when more layers exist in many of these financial restructurings. The current crisis is part of a business cycle and its swings can only be damped by government or regulatory intervention. The Minskian view is also supported by recent publications before the credit crunch. For example, Sornette proposed models in which a speculative bubble builds up in months or even years before the crisis, rather than describing a mechanism operating at short time scales of hours, days or weeks at most

[1] Correspondence could be addressed to:
Email: Marco.van.der.Burgt@gmail.com

[Sornette2003]. Considering the credit crisis as part of a business cycle, how does this cycle influence validation of the PD?

The requirement that the PD must be an average over the business cycle has consequences for the validation of PD rating models [Basel2005]. In the validation process, the recently observed 1-year default rate is compared with the PD scale, which is a long-term average of default rates. This means that the 1-year default rate will be lower than the PD in an upturn of the economy and the conclusion of the validation exercise might be that the model is too conservative. On the other hand, the 1-year default rate will be higher than the PD in a downturn of the economy, and the model is perceived as too optimistic. As such, two important questions should be addressed in the validation exercise:

1. How long is the business cycle?
2. Where exactly are we in the business cycle?

The answer to both questions can be used by making a business cycle adjustment on the recently observed default rate before this default rate is compared with the PD, which is an average over the business cycle.

This paper focuses on answering the two questions by applying Fourier analysis and wavelet analysis. Since Fourier analysis reveals the frequencies in a time series, this technique is eligible to answer the first question on the duration of a business cycle. By Fourier transforming from time to frequency space, localization is lost and the second question can not be answered. In addition, it is assumed that the period of a business cycle will always be the same through time.

Over the last 3 decades, a new technique is introduced and called wavelet analysis. Wavelet analysis is essentially a transformation from time space to the time-frequency domain. As such, wavelet analysis transforms a time series into an image of time versus frequency and it might identify the period of a business cycle and in which phase of the business cycle we are in.

In this paper we apply Fourier and wavelet analysis on a time series of monthly observed default rates. The paper will report on the results and is organized as follows. In the next section, the results of the Fourier analysis are presented. Section 3 introduces the concept of wavelets as a tool for transforming time series in the time-frequency domain. Section 4 describes a version of the wavelet transform known as the Maximum Overlap Discrete Wavelet Transform. The results of the wavelet analysis are described in section 5 and section 6 concludes. Table 1 gives an overview of the mathematical symbols used.

2. Fourier analysis of Business Cycles

A traditional method to estimate a frequency from a signal or time series is Fourier analysis [Folland1992]. A time series X_t is Fourier transformed into frequency space by the following equation:

$$\tilde{X}_k = \frac{1}{N}\sum_{t=1}^{n} X_t \exp\left\{2pi\frac{kt}{N}\right\}$$

Equation 2-1

where the Fourier component $\tilde{X}_k$ is a complex coefficient which shows the relative contribution of the frequency k / N to the time series. The estimation of periodicity is based on searching the Fourier component with the largest power $\left|\tilde{X}_k\right|^2$.

Fourier analysis is applied on monthly observed default rates, which are available from Standard & Poor's (S&P) CreditPro® v7.02 database. We preferred monthly observed default rates rather than annual default rates in order to obtain more data and a much more accurate estimation of the business cycle period. The data, which are shown in Figure 1, cover the period from 1981 to 2007. Figure 2 shows the Fourier power $\left|\tilde{X}_k\right|^2$ as a function of the frequency in reciprocal years. The figure reveals that the maximum power occurs at a frequency of 0.09 years^{-1}, which corresponds to a period of 10.67 years. Figure 1 also shows the fit of the monthly default rate to a sine function with a frequency of 0.9 years^{-1}.

The Fourier analysis of the time series of monthly observed default rates gives an answer to the first question: how long is a business cycle? According to the analysis, this is 10.67 years. However, information on localization in time is lost in Fourier analysis, because of transformation from time space to frequency space. In addition, in Fourier analysis it is assumed that the frequency content in the time series is stationary, whereas the period of a business cycle might change through history.

3. Wavelet analysis

Unlike the harmonic functions in the Fourier transform, wavelets are functions with localization both in time and in scale, thereby providing a convenient way of representing complex signals and time series. Therefore, it is not surprising that wavelets are frequently applied in physics, signal processing and time series analysis (see [von Sachs1996, Moulin1994, Percival2000]). In addition, wavelet theory is also applied in non-parametric regression and density estimation [Antoniadis1995], data compression, solving differential equations [Mattos2003, Lepik2005] and inverse problems like singular value decomposition [Donoho1995]. A detailed treatment of wavelet theory is beyond the scope of this paper, but a concise introduction will be presented here. The reader is referred to literature elsewhere for a more elaborate description of wavelets [Percival2000, Daubechies1992, Chui1992].

A wavelet is a function with the following properties:

$$\int_{-\infty}^{\infty} \psi(x)\,dx = 0$$

$$\int_{-\infty}^{\infty} [\psi(x)]^2\,dx = 1$$

Equation 3-1

Figure 3 exhibits two examples of wavelet functions, the block-shaped Haar wavelet, hereafter denoted as ψ^H, and the shark-fin shaped Daubechies-4 wavelet, hereafter denoted as ψ^D [Daubechies1992]. Both wavelets show an upward movement, followed by a downward movement. As such, both wavelets resemble the behaviour of default rates through the cycle: in a downturn of the business cycle the default rates will rise, and in an upturn of the cycle, the default rates will fall. Identifying the business cycle by an economic downturn with increasing default rates, followed by an economic upturn with declining default rates, the duration of the business cycle and location in the business cycle might be revealed by dilating and translating the wavelet function to obtain a maximum overlap between the wavelet function and the default rate time series. This is in essence the key of the analysis.

A wavelet function $\psi(x)$ can be dilated over a time interval τ and translated over a time t by defining a new wavelet function:

$$\psi_{\tau,t}(x) = \frac{1}{\sqrt{\tau}}\psi\left(\frac{x-t}{\tau}\right)$$

Equation 3-2

Note that $1/\sqrt{\tau}$ results from the normalization condition as given in Equation 3-1. The overlap between a function f(x) and $\psi_{\tau,t}(x)$ is calculated as

$$W(\tau,t) = \int_{-\infty}^{\infty} f(x)\cdot\psi_{\tau,t}(x)\,dx = \langle f, \psi_{\tau,t}\rangle$$

Equation 3-3

where $W(\tau, t)$ is the wavelet coefficient and <,> denotes the inner product. Equation 3-3 is known as the continuous wavelet transformation (CWT). When the wavelets $\psi_{\tau,t}(x)$ are orthonormal, they form a basis for the function space and every function f(x) can be decomposed as a linear combination of wavelet functions $\psi_{\tau,t}(x)$.

The wavelet transformation in Equation 3-3 assumes that the function f(x) is continuous. However, most time series X_t are sampled as discrete values at times t = 0, 1, …, N-1 and consist of a finite sequence of length N.

Therefore, a discrete version of the wavelet transform, known as the Discrete Wavelet Transformation (DWT), is introduced by standardizing τ to a dyadic scale: $\tau_j = 2^j$. In addition, a wavelet basis is introduced, which consists of a father wavelet[2] $\varphi_{j,t}$ that represents the smooth baseline trend and a mother wavelet $\psi_{j,t}$ that is dilated and shifted to construct different levels of detail:

$$j_{j,t}(x) = \frac{1}{2^{j/2}} j\left(\frac{x-t}{2^j}\right)$$

$$y_{j,t}(x) = \frac{1}{2^{j/2}} y\left(\frac{x-t}{2^j}\right)$$

Equation 3-4

As a short example, a time series of 4 discrete values X_t ($t = 0, 1, 2, 3$) is considered and decomposed in Haar wavelets, for which $\varphi^H(x)$ equals 1 in the interval (0, 1) and zero otherwise and $\psi^H(x)$ is 1 on interval (0, ½), -1 on interval (1/2, 1) and zero otherwise. The time series x_t can be decomposed in normalized Haar wavelets as follows:

$$\begin{bmatrix} x_0 \\ x_1 \\ x_2 \\ x_3 \end{bmatrix} = \frac{x_0 + x_1 + x_2 + x_3}{2} \cdot \frac{1}{2} \begin{bmatrix} 1 \\ 1 \\ 1 \\ 1 \end{bmatrix} + \frac{x_0 + x_1 - x_2 - x_3}{2} \cdot \frac{1}{2} \begin{bmatrix} 1 \\ 1 \\ -1 \\ -1 \end{bmatrix} + \frac{x_0 - x_1}{\sqrt{2}} \cdot \frac{1}{\sqrt{2}} \begin{bmatrix} 1 \\ -1 \\ 0 \\ 0 \end{bmatrix} + \frac{x_2 - x_3}{\sqrt{2}} \cdot \frac{1}{\sqrt{2}} \begin{bmatrix} 0 \\ 0 \\ 1 \\ -1 \end{bmatrix}$$

$$= V_{2,0} \cdot j_{2,0}^{H} + W_{2,0} \cdot y_{2,0}^{H} + W_{1,0} \cdot y_{1,0}^{H} + W_{1,2} \cdot y_{1,2}^{H}$$

Equation 3-5

where the wavelet coefficients are calculated as $W_{j,t} = \langle x_t, \psi^H_{j,t} \rangle$ and $V_{j,t} = \langle x_t, \varphi^H_{j,t} \rangle$ respectively. Two features emerge from the example: first, these coefficients consist of successive averaging and differencing observations. Since averaging corresponds to filtering out high frequencies and differencing corresponds to filtering out low frequencies, DWTs are often described in terms of low-pass filters and high pass filters, leading to recursive equations for the wavelet coefficients [Mallat1989, Percival2000]. Secondly, Equation 3-5 shows that the wavelet functions $\varphi^H_{2,0}$, $\psi^H_{2,0}$, $\psi^H_{1,0}$ and $\psi^H_{1,2}$ are orthonormal and therefore span the space of observed time series X_t.

4. Maximum Overlap Discrete Wavelet Transform

The orthonormality in the DWT imposes restrictions: the number of observations must be a power of two. In addition, the DWT algorithm removes values from the observations, which is frequently referred to a down-sampling. Another drawback of the DWT is that it is not translation invariant. Therefore, a non-orthonormal version of the DWT, known as the Maximum Overlap Discrete Wavelet Transform (MODWT), is applied in this paper. Unlike the DWT, the MODWT can be applied to all sample sizes and is translation invariant. The MODWT technique is also known as the non-decimated DWT, redundant DWT, translation-invariant DWT or stationary DWT.

We use two types of wavelets, the Haar wavelet and the Daubechies-4 wavelet, because both functions are characterized by an upward swing and a downward swing and that makes them eligible for identifying business cycles by finding maximum overlap. As shown in the example of section 3, the calculation of wavelet coefficients corresponds to filtering. The Haar wavelet filter has a length L = 2 and filter coefficients

$$h_0 = \frac{1}{\sqrt{2}}, h_1 = -\frac{1}{\sqrt{2}}$$

Equation 4-1

The Daubechies-4 wavelet filter has a length L = 4 [Daubechies1992] and filter coefficients:

[2] The father wavelet is also called the scaling function.

$$h_0 = \frac{1-\sqrt{3}}{4\sqrt{2}},\ h_1 = \frac{-3+\sqrt{3}}{4\sqrt{2}},\ h_2 = \frac{3+\sqrt{3}}{4\sqrt{2}},\ h_3 = \frac{-1-\sqrt{3}}{4\sqrt{2}}$$

Equation 4-2

The wavelet filter coefficients h_l and associated scaling filter coefficients g_l are related by the following equation [Daubechies1992, Chui1992, Mallat1989, Percival2000]:

$$g_l = (-1)^{l-1} h_{L-1-l}$$

Equation 4-3

The filtering approach leads to a recursion algorithm to calculate the wavelet coefficients. In case of the MODWT, it will be shown in the appendix that the MODWT wavelet coefficients are easily calculated by the following recursive equations

$$V_{j,t} = \sum_{l=0}^{L-1} g_l V_{j-1,t+2^{j-1}l \bmod N}$$

$$W_{j,t} = \sum_{l=0}^{L-1} h_l V_{j-1,t+2^{j-1}l \bmod N}$$

Equation 4-4

where $V_{0,t} = X_t$ and g_l and h_l are so-called filter coefficients. The operation *k mod N* is equivalent to *k modulo N* and is defined as *m mod N = m* if $0 \le k \le N-1$, otherwise *m mod N = k+nN* with n as a unique integer yielding $0 \le k+nN \le N-1$. The effect of the *k mod N* operation is that the signal is periodized, for example X_{-1} becomes X_{N-1}, X_{-2} becomes X_{N-2}, etc. We will denote vectors with wavelet coefficients $V_{j,t}$ and $W_{j,t}$ as W_j and V_j respectively.

The resulting wavelet coefficients $V_{j,t}$ and $W_{j,t}$ represent the overlap of the time series X_t with the functions $\varphi_{j,t}$ and $\psi_{j,t}$ respectively. The Daubechies-4 and Haar wavelet functions $\psi_{j,t}$ are shown for j = 3 and t = 5 in Figure 3. Figure 3 shows that although both wavelets have the same scaling and translation, their width and the start of the upward movement is different[3]. Whereas the Haar wavelet directly moves up at t = 5, the Daubechies-4 wavelet starts at t = 13. In general, the Daubechies-4 wavelet starts to move up at $t + 2^j$ at level j, whereas the Haar wavelet immediately moves up at time t. This "offset" of 2^j must be taken into account when the overlap of the time series with ψ^H and ψ^D are compared. Therefore, the time t is transformed by the following operation in case of the Daubechies-4 wavelet:

$$t \to \{t + 2^j\} \bmod N$$

Equation 4-5

Once the coefficients $W_{j,t}$ are calculated up to a certain level J, the periodicity of the business cycle can be derived from j and the start of the business cycle is derived from t by searching for the largest wavelet coefficient $W_{j,t}$. This coefficient is the maximum overlap between the wavelet function and the time series.

5. Wavelet analysis of default rates

The MODWT is applied in analyzing the time series X_t (t = 0, 1, 2, …) of monthly default rates of S&P CreditPro® v7.02 database. This data consists of 324 observations, which cover the period from year 1981 to 2007. Wavelet coefficients $W_{j,t}$ are calculated by applying Equation 4-4 and using $V_{0,t} = X_t$.

In the analysis, the period of the business cycle and start of the business cycle is identified by finding the values of j and t of the maximum wavelet overlap $W_{j,t}$. However, the time series contains a considerable amount of noise as shown in Figure 1. Therefore, the variance in the default rates is not only explained by business cycles, but also by noise, which questions to what extend both noise and business cycles contribute to the total variance of default rates. Fortunately, wavelet analysis allows a decomposition of variance at different time scales. It can

---

[3] In general, the width of a wavelet at scale j with filter length L equals [Percival2000]: $L_j = (2^j - 1)(L-1) + 1$. One might define an effective width as 2^j, which is the width between the start from the upward movement to the end of the downward movement. In case of the Haar wavelet, the effective width equals L_j.

be shown that the variance of time series X can be expressed in wavelet coefficients by the following equation [Percival2000]:

$$s_X^2 = \sum_{j=1}^{J} \frac{1}{N} \left| W_j \right|^2 + \frac{1}{N} \left| V_J \right|^2 - \langle X \rangle^2$$

Equation 5-1

where W_j and V_j are vectors with wavelet coefficients $W_{j,t}$ and $V_{j,t}$ respectively and <X> is the average default rate. Level j ranges from 1 to J, where J is chosen as the floor integer value of N / 2^J, which gives J = 8. Equation 5-1 shows that every level j contributes by an amount of $\frac{1}{N} \left| W_j \right|^2$ to the total variance σ_X^2 of X. This contribution is often referred to as the energy of the time series at level j [Percival2000].

Table 2 presents the contribution of every level to the total variance σ_X^2 in percentages of the total variance. The contribution is shown graphically by the energy spectrum in Figure 4. The highest contribution is observed for j = 1, which corresponds to the highest frequency component and is therefore attributed to noise. The energy at level j = 7 also gives a large contribution. Since this level corresponds to the frequency of a business cycle, this component is interpreted as the business cycle part of the variance. Level j = 7 corresponds to a period of 2^7 months, which equals 10.67 years and is therefore in agreement with the Fourier analysis as exhibited in Figure 2. The business cycle contribution in case of the Daubechies-4 wavelet analysis is larger than the business cycle contribution in case of the Haar wavelet analysis. This leads to the conclusion that Daubechies-4 wavelets are more eligible to filter out business cycles from a noisy time series than Haar wavelets. Another significant contribution to the variance is observed for level j = 6. This contribution amounts to 16.67% in case of the Haar wavelets and 17.83% in case of the Daubechies-4 wavelets. An investigation on the maximum wavelet coefficients for j = 6 reveals that this is caused by the spikes, which are observed in January 1991, December 2001 and March 2002.

After identifying the periodicity of the business cycle by Fourier analysis and MODWT, the next step is to find out the start of the business cycle by searching for maxima in the wavelet coefficients $W_{j,t}$ for j = 7. These coefficients are presented in Figure 5 for both the Haar and Daubechies-4 wavelets. In this figure, the transformation in Equation 4-5 is applied to t in case of the Daubechies-4 wavelet, in order to account for the offset as mentioned in section 4.

The Haar wavelets show maximum overlap at t1 = 83 and t2 = 209, which corresponds to December 1987 and June 1998 respectively. Therefore, the Haar analysis reveals two business cycles, one starting at December 1987 and one starting at June 1998. Each business cycle starts with an economic downturn, characterized by a high default rate. As the business cycle has a duration of 128 months, the first cycle ends at July 1998 and the second one at January 2009.

The Daubechies-4 analysis also reveals two business cycles, but these cycles start at t1 = 63 and t2 = 199 respectively. These time stamps correspond to April 1986 and August 1997 respectively. Comparing the $W_{j,t}$ coefficients of Haar wavelets and Daubechies-4 wavelets in Figure 5 shows that the series of coefficients in case of Daubechies-4 wavelets is less noisy than in case of Haar wavelets. Given that the business cycle has a duration of 128 months, the first cycle matures at November 1996 and the second cycle matures at March 2008.

The discrepancy in the starting points between the Haar wavelets and Daubechies-4 wavelets is explained by their different shapes. The shark-fin shaped Daubechies-4 wavelet matches the default rates much better than the blocky Haar wavelets. Since the Daubechies-4 wavelets are more capable of filtering out the underlying cycles than the Haar wavelets, the Daubechies-4 wavelet is considered more reliable.

We investigated further how well a wavelet with maximum overlap approximates the original time series. The time series of default rates is compared with the following approximation:

$$X_{approx} = \langle X \rangle + W_{j,t1} y_{j,t1} + W_{j,t2} y_{j,t2}$$

Equation 5-2

In this approximation, <X> is the average of the default rates, j = 7 and t1 and t2 refer to the time values at which maximum overlap is observed respectively. Figure 6 compares the approximation in Equation 5-2 with the time series in case of the Haar wavelets, whereas Figure 7 gives the comparison in case of the Daubechies-4 wavelets. In order to quantify to what extend the approximation mimics the time series of default rates, we define average deviation (AD) between the time series X_t and the approximation in Equation 5-2 as:

$$AD = \left\{ \frac{1}{N} \sum_t \left(X_{approx,t} - X_t \right)^2 \right\}$$

Equation 5-3

The AD equals $1.17 \cdot 10^{-3}$ in case of the Haar wavelet and $1.16 \cdot 10^{-3}$ in case of the Daubechies-4 wavelet. Based on the smallest AD, it is concluded that the Daubechies-4 wavelet has a better overlap with the default rates than the Haar wavelet.

Since the noise contribution in the total variance is quite large and amounts to 20% of the variance, one might wonder how this influences the outcomes of the results in the previous sections. Therefore, a Multi-Resolution Analysis (MRA) is applied to the time series of monthly default rates. The MRA is a representation of the time series at different time resolutions, thereby filtering out high-frequency components like noise at coarse time resolutions. The MRA is described briefly in the appendix, which shows that the time series will be decomposed into the following components:

$$X = \sum_{j=1}^{J} D_j + S_J$$

Equation 5-4

The components D_j are called wavelet "details" as they capture local fluctuations over the whole period of time at each scale j. The component S_J provide a "smooth" or overall "trend" of the original time series X. Adding D_j to S_J for j = 1, 2, …, J gives an increasingly more accurate approximation of the original signal. The interested reader can find more extensive background literature elsewhere [Mallat1989, Percival2000].

Based on the conclusion that Daubechies-4 wavelets are more eligible to filter out business cycles from noisy time series than Haar wavelets, a MRA using Daubechies-4 wavelets is applied up to level J = 3 and shown in Figure 8. The figure shows how the time series X is decomposed in high-frequency components D_1, D_2 and D_3 and a smoothed component S_3, which is less noisy than the original time series. This noise reduction in S_3 is also supported by comparing the energy spectrum of S_3 with the energy spectrum of the original time series, as shown in Figure 9. The figure shows that the high frequency components at level 1, 2 and 3 are filtered out in the S_3 spectrum and as a result level j = 7 contributes to 38.49% of the total variance. Thus S_3 is a smoothed version of the time series X. Calculation of the wavelet coefficients $W_{j,t}$ of the smoothed time series X and identifying the value of t at which $W_{j,t}$ has a maximum reveals no differences with the values of the original time series.

Based on the wavelet analysis of monthly default rates, the last cycle ends at March 2008 and we are currently in the downturn of a new business cycle, which is clearly apparent in the ongoing credit crisis. However, as mentioned in the introduction, we consider the collapse in the credit markets as a business cycle event, which is triggered by failure of mortgage companies, the bubble in the U.S. housing market, complexity of new financial instruments and incorrect risk perception of mortgage-backed securities (for a review on the causes of the credit crisis, see [Steverman2008]). Instead of learning from the collapse of the technology bubble in the beginning of the 21th century, the roots of the crisis started in this period with declining lending standards, increasing loan incentives and rising of housing prices. In addition to the business cycle effect, we also investigated whether there is an upward tendency by decomposition of the time series of default rates up to level 8. Figure 10 shows the smoothed component S_8, which shows a periodicity of 10.67 years, superposed on a slight increase in default rates. A linear regression of S_8 versus t shows that this increase amounts to 0.0017% per year, which is not considered significant.

6. Conclusion

This paper presents a wavelet analysis of business cycles, based on S&P default rates. The analysis is used to address the following questions: how long is a business cycle and where are we in the business cycle?
Both Fourier analysis and wavelet analysis of the monthly observed S&P default rates reveal a business cycle of 10.67 years. The location in the business cycle can not be answered by Fourier analysis, but analysis with Haar wavelets shows two business cycles, one with a downturn starting at December 1987 and maturing at July 1998 and one starting with a downturn at June 1998 and maturing at January 2009.
The Daubechies-4 analysis also shows two business cycles in the data, one starting with a downturn at April 1986 and maturing at November 1996, and one starting with a downturn at August 1997 and maturing at March 2008. Analysis with Daubechies-4 wavelets gives more precision than in case of Haar wavelets. This conclusion is supported by the variance decomposition by Haar and Daubechies-4 wavelets, which shows that Daubechies-4 wavelets are more eligible to filter out business cycles from a noisy time series than Haar wavelets. Based on the Daubechies-4 wavelet analysis, currently we are in the economic downturn of a new business cycle. Of course this is an understatement, given the current financial crisis. However, the credit crisis is considered as caused by the rising of U.S house prices at unsustainable levels, risky securitization deals and increasing complexity of financial instruments. These underlying factors can not be revealed alone by time series analysis, but require a structural modelling approach.

Knowing the start and the period of the business, this should be regarded in validating the PDs by comparing them with the actually observed 1-year default rate. A possible approach to include business cycle effects in PD validation is to multiply the observed 1-year default rate by a cycle adjustment factor, before the 1-year default rate is compared with the PD. A cycle adjustment factor (CA) can be defined as a scaling factor, which “scales up” the observed 1-year default rate to a long-term average:

$$CA = \frac{d_{cycle}}{d_t}$$

Equation 6-1

In this equation, d_{cycle} is the 1-year default rate, observed and averaged over the business cycle, and d_t is the currently observed 1-year default rate. An alternative is the Odds-Ratio Scalar Method [Hodges2008]. Other approaches are also under study, for example Miu et al. present a method to enhance historical default data using the default history of external ratings [Miu2007].

7. Appendix: Mathematics of the MODWT algorithm

This appendix provides a mathematical background of the MODWT by deriving equations for the wavelet coefficients and multi-resolution analysis. We will use the symbol ^ for matrices and the brackets <,> as inner product between vectors.

The wavelet coefficients represent the overlap between the time series and the wavelet:

$$V_{j,t} = \langle \varphi_{j,t}, f \rangle = \int_{-\infty}^{\infty} \varphi_{j,t}(x) f(x) dx$$

$$W_{j,t} = \langle \psi_{j,t}, f \rangle = \int_{-\infty}^{\infty} \psi_{j,t}(x) f(x) dx$$

Equation 7-1

where the father and mother wavelet are defined as in Equation 3-4. A basic property of wavelets is that the scaling function φ satisfies the dilation equation [Chui1992, Mallat1989]:

$$\varphi(x) = \sum_{l=0}^{L-1} g_l \varphi(2x - l)$$

Equation 7-2

This equation relates the scaling function at two successive scales by the filter coefficients g_l, hence it is also referred to as the two-scale equation or refinement equation. A similar equation exists for the mother wavelet function ψ with filter coefficients h_l:

$$\psi(x) = \sum_{l=0}^{L-1} h_l \varphi(2x - l)$$

Equation 7-3

In order to find the wavelet coefficients by Equation 7-1, the father and mother wavelet functions have to be found by solving the dilation equations numerically. Although there are different ways to solve the dilation equations like iteration and Fourier transformation [Strang1989], the wavelet coefficients are more interesting than the solutions itself. The wavelet coefficients can be found directly without solving the dilation equations by casting the dilation equations in the following form:

$$\varphi_{j,t}(x) = 2^{-j/2}\varphi\left(\frac{x-t}{2^j}\right) = \sum_{l=0}^{L-1} g_l 2^{-j/2}\varphi\left(\frac{x-t}{2^{j-1}} - l\right) = \sum_{l=0}^{L-1} g_l 2^{-j/2}\varphi\left(\frac{x-t-2^{j-1}l}{2^{j-1}}\right) = \sum_{l=0}^{L-1} 2^{-1/2} g_l \varphi_{j-1,t+2^{j-1}l}(x)$$

$$\psi_{j,t}(x) = 2^{-j/2}\psi\left(\frac{x-t}{2^j}\right) = \sum_{l=0}^{L-1} h_l 2^{-j/2}\varphi\left(\frac{x-t}{2^{j-1}} - l\right) = \sum_{l=0}^{L-1} h_l 2^{-j/2}\varphi\left(\frac{x-t-2^{j-1}l}{2^{j-1}}\right) = \sum_{l=0}^{L-1} 2^{-1/2} h_l \varphi_{j-1,t+2^{j-1}l}(x)$$

Equation 7-4

Combining Equation 7-1 to Equation 7-4 leads to a recursive relation between the wavelet coefficients:

$$V_{j,t} = \sum_{l=0}^{L-1} 2^{-1/2} g_l V_{j-1,t+2^{j-1}l}$$

$$W_{j,t} = \sum_{l=0}^{L-1} 2^{-1/2} h_l V_{j-1,t+2^{j-1}l}$$

Equation 7-5

Equation 7-5 can be written in matrix form by introducing matrices $\hat{A}$ and $\hat{B}$:

$$V_j = \hat{A}_j V_{j-1}$$

$$W_j = \hat{B}_j V_{j-1}$$

Equation 7-6

In this equation, V_j and W_j are vectors. Using the iteration in Equation 7-6, the relationship between coefficient vectors V_j and W_j and time series X can be written in matrix form:

$$V_j = \hat{A}_j \hat{A}_{j-1} \ldots \hat{A}_2 \hat{A}_1 V_0 = \hat{\mathrm{V}}_{\mathrm{j}} V_0 = \hat{\mathrm{V}}_{\mathrm{j}} X$$

$$W_j = \hat{B}_j \hat{A}_{j-1} \ldots \hat{A}_2 \hat{A}_1 V_0 = \hat{\mathrm{W}}_{\mathrm{j}} V_0 = \hat{\mathrm{W}}_{\mathrm{j}} X$$

Equation 7-7

Based on Equation 7-7, time series X can be decomposed in a J-level smoothed time series $\mathrm{S_J} = \hat{\mathrm{V}}_{\mathrm{J}}^{\mathrm{T}} V_J = \hat{\mathrm{V}}_{\mathrm{J}}^{\mathrm{T}} \hat{\mathrm{V}}_{\mathrm{J}} X$ and j-level details $\mathrm{D_j} = \hat{\mathrm{W}}_{\mathrm{j}}^{\mathrm{T}} W_j = \hat{\mathrm{W}}_{\mathrm{j}}^{\mathrm{T}} \hat{\mathrm{W}}_{\mathrm{j}} X$:

$$X = \sum_{j=1}^{J} D_j + S_J$$

Equation 7-8

Equation 7-8 is basically the calculation of the multi-resolution analysis. The components D_j present the wavelet details at scale j and the component S_J is a smoothing of the time series X. Equation 7-8 reveals that the original time series can be reconstructed by adding the detail components D_j to the smoothed time series S_J.

REFERENCES

[Antoniadis1995] A. Antoniadis, G. Oppenheim (Eds.), *Wavelets and statistics*, Lecture notes in statistics 103, New York: Springer-Verlag

[Basel2004] Basel Committee on Banking Supervision, *International Convergence of Capital Measurement and Capital Standards, A Revised Framework*, July 2004

[Basel2005] Basel Committee on Banking Supervision, *Studies on the Validation of Internal Rating Systems*, revised version, May 2005

[Chui1992] C.K. Chui, *An Introduction to Wavelets*, Academic Press Professional ISBN:0-12-174584-8, (1992)

[Daubechies1992] I. Daubechies, *Ten Lectures on Wavelets*, Philadelphia, SIAM.

[Donoho1995] D.L. Donoho, *Nonlinear solution of linear inverse problems by wavelet-vaguelette decomposition*, Appl. Comput. Harm. Anal. 2 (1995) p. 101-126

[Folland1992] G. B. Folland, *Fourier Analysis and Its Applications*, Brooks/Cole Publishing Co., 1992

[Hodges2008] P.A.B. Hodges, *Danske Bank Group's TTC PD Transformation Process*, Eurobanking (2008).

[Lepik2005] Ü. Lepik, *Numerical solution of differential equations using Haar wavelets*, Mathematics and Computers in Simulation, Vol. 68 No.2, (2005), p. 127 - 143

[Mallat1989] S.G. Mallat, *A theory for multiresolution signal decomposition: the wavelet presentation*, IEEE Trans. Pattn. Anal. Mach. Intell. 11 (1989) p. 674-693

[Mattos2003] J.R. Linhares de Mattos, E.P. Lopes, *A wavelet Galerkin method applied to partial differential equations with variable coefficients*, Fifth Mississippi State Conference on Differential Equations and Computational Simulations, Electronic Journal of Differential Equations, Conference 10, 2003, pp 211–225.

[Minsky1985] H.P. Minsky, *The Financial Instability Hypothesis: A Restatement*, Post Keynesian Theory: A Challenge to Neo Classical Economics. P. Arestis, T. Skouras (eds.), (1985)

[Minsky1986] H.P. Minsky, *Stabilizing an Unstable Economy*, McGraw-Hill Companies, 1986

[Minsky1993] H.P. Minsky, *The Financial Instability Hypothesis*, Working Paper No. 74. Annandale-on-Hudson: Jerome Levy Economics Institute. Reprinted in Philip Arestis and Malcolm Sawyer (eds.), Handbook of Radical Political Economy, (1993). Paper can be downloaded at www.levy.org/pubs/wp74.pdf.

[Miu2007] *P. Miu, B. Ozdemir, Estimating and Validating Long-Run Probability of Default with respect to Basel II Requirements*, J. Risk Model Validation, to be published (2007).

[Moulin1994] *Wavelet thresholding techniques for power spectrum estimation*. IEEE Trans. Sig. Proc. 42 (1994) p. 3126-3136

[Percival2000] D.B. Percival, A.T. Walden, *Wavelet Methods for Time Series Analysis*, Cambridge University Press, 2000 ISBN 0521640687, 9780521640688

[von Sachs1996] R. von Sachs, *Adaptively wavelet-smoothed Wigner estimates of evolutionary spectra*. Z. Angew. Math. Mech., 76 (1996) p. 71-74

[Sornette2003] D. Sornette, *Critical Market Crashes*, Physics Reports Vol. 378(1), April 2003, p.1-98

[Steverman2008] B. Steverman, D. Bogoslaw, *The Financial Crisis Blame Game*, Business Week, October 18, 2008

[Strang1989] G. Strang, *Wavelets and Dilation Equations: A Brief Introduction,* SIAM Review, Vol. 31, No. 4. (1989), p. 614-627.

[Strang1993] G. Strang, *Wavelet transforms versus Fourier transforms*, Bull. (New Series) Am. Math. Soc. 28 (1993) p. 288-305

Symbol	Description
X	Time series of monthly default rates
X_t	Observation at time t of time series X
$\tilde{X}_k$	Fourier transform of X_t
<X>	Average of time series X
$\psi^H_{j,t}$	Haar mother wavelet at level j and starting at time t
$\varphi^H_{j,t}$	Haar father wavelet at level j and starting at time t
$\psi^D_{j,t}$	Daubechies-4 mother wavelet at level j and starting at time t
$\varphi^D_{j,t}$	Daubechies-4 father wavelet at level j and starting at time t
$V_{j,t}$	Father wavelet coefficient at level j and time t
$W_{j,t}$	Mother wavelet coefficient at level j and time t
V_j	Vector of father wavelet coefficients at level j
W_j	Vector of mother wavelet coefficients at level j
$\|W_j\|^2$	Energy at level j
$\hat{V}_j$	Matrix for transforming time series X into vector V_j
$\hat{W}_j$	Matrix for transforming time series X into vector W_j
σ_X^2	Variance of time series X

Table 1 Summary of mathematical symbols

Level	Time scale (years)	% of variance, decomposition based on Haar Wavelets	% of variance, decomposition based on Daubechies-4 wavelets.
1	0.17	23.55%	23.43%
2	0.33	12.71%	12.11%
3	0.67	9.19%	8.77%
4	1.33	7.56%	6.12%
5	2.67	10.19%	8.42%
6	5.33	16.67%	17.83%
7	10.67	16.59%	20.60%
8	21.33	2.23%	2.26%
$\frac{1}{N}\|V_J\|^2 - \langle X \rangle^2$	21.33	1.30%	0.47%

Table 2 Decomposition of variance in default rates at different time scales. Level j = 7 corresponds to the business cycle component of the total variance. The largest contribution is observed for level j = 1, which is interpreted as the noise contribution to the variance in default rates.

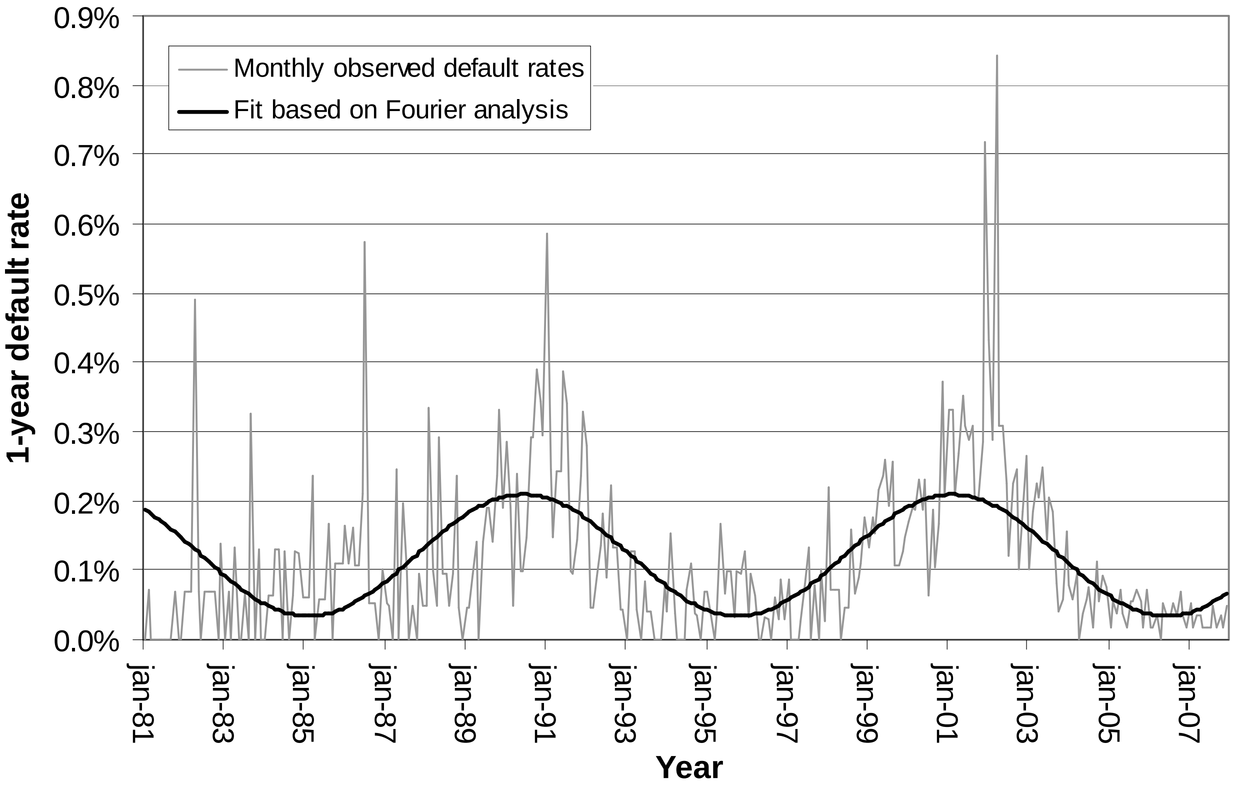

Figure 1 Time series on monthly observed default rates over the period from 1981 to 2007. The sinusoidal fit is based on Fourier analysis. *Source*: Standard & Poor's CreditPro® v7.02, (https://creditpro.standardandpoors.com/)

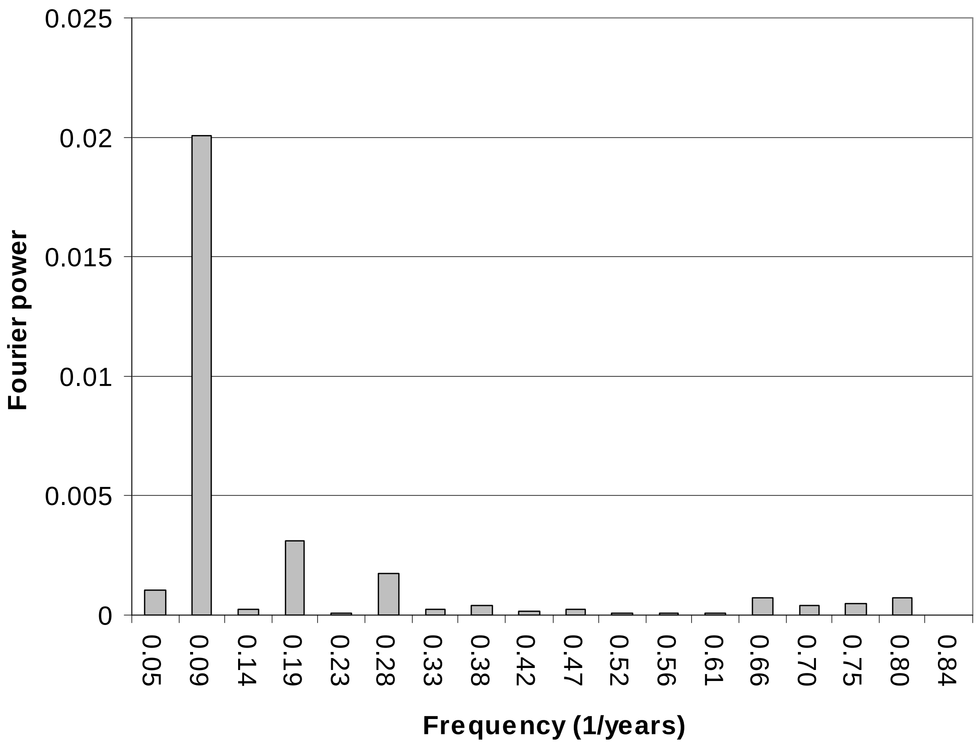

Figure 2 Fourier power spectrum, resulting from the Fast Fourier Transform of monthly default rates. The highest power is observed for a frequency of 0.09, which corresponds to a period of 10.67 years.

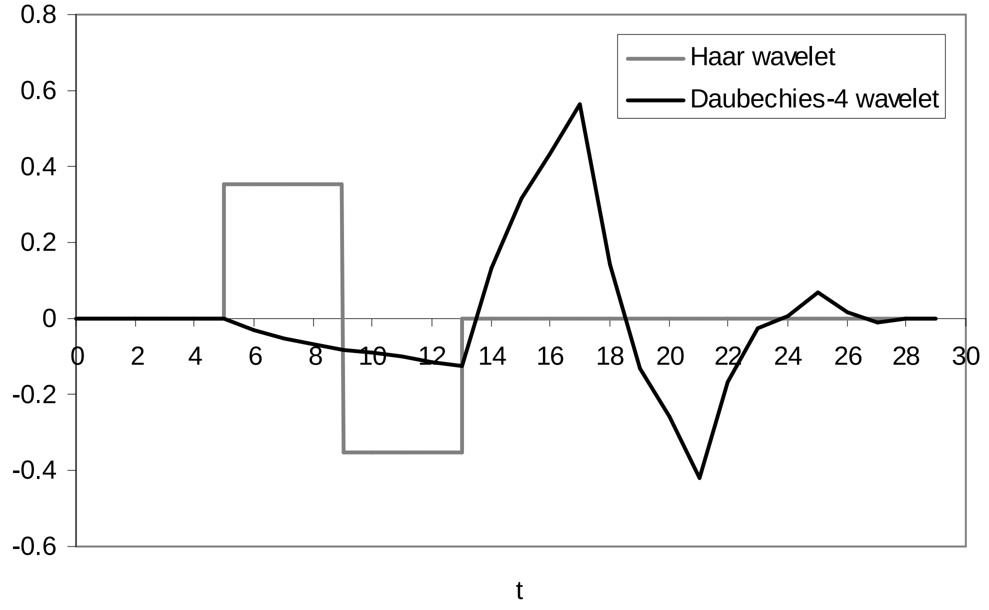

Figure 3 Haar wavelet $\psi^{H}_{j,t}$ and Daubechies-4 wavelet $\psi^{D}_{j,t}$, depicted for j = 3 and t = 5.

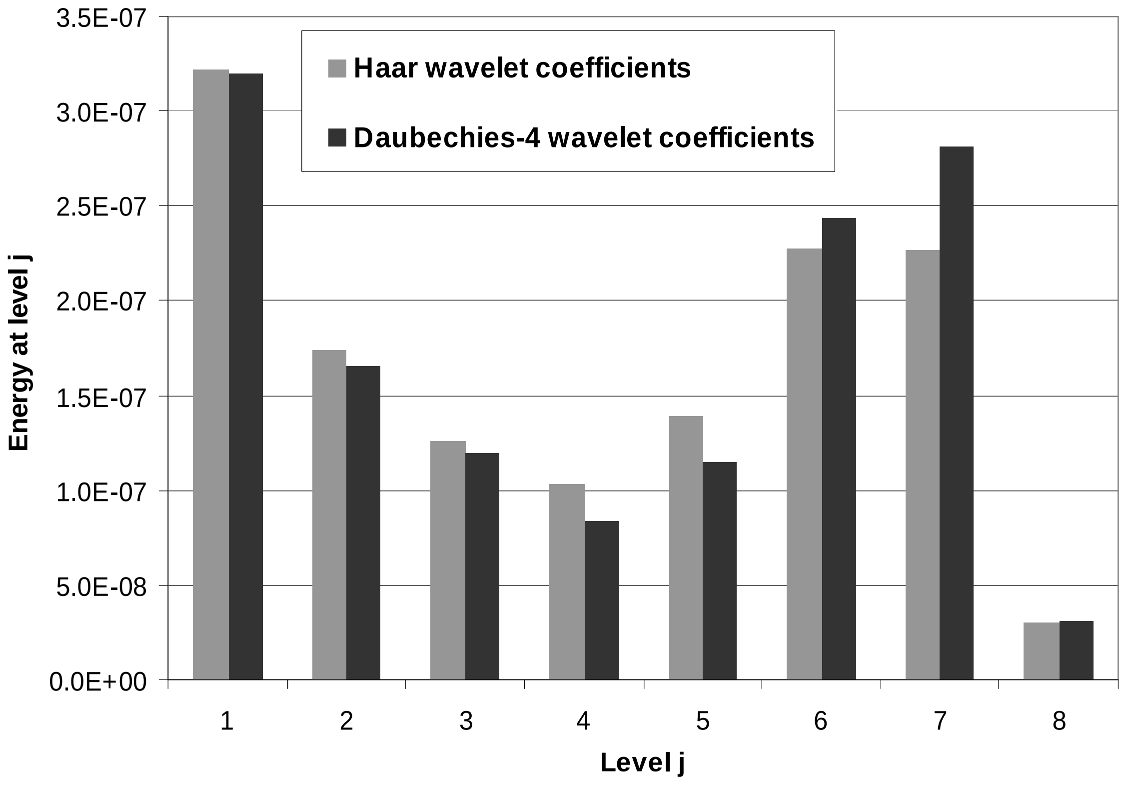

Figure 4 Energy spectrum of wavelet coefficients as a function of resolution level j. The energy at j = 1 is attributed to noise. With exception for j = 1, the maximum energy is observed for level j = 7, which corresponds to a period of 2^7 months (10.67 years)

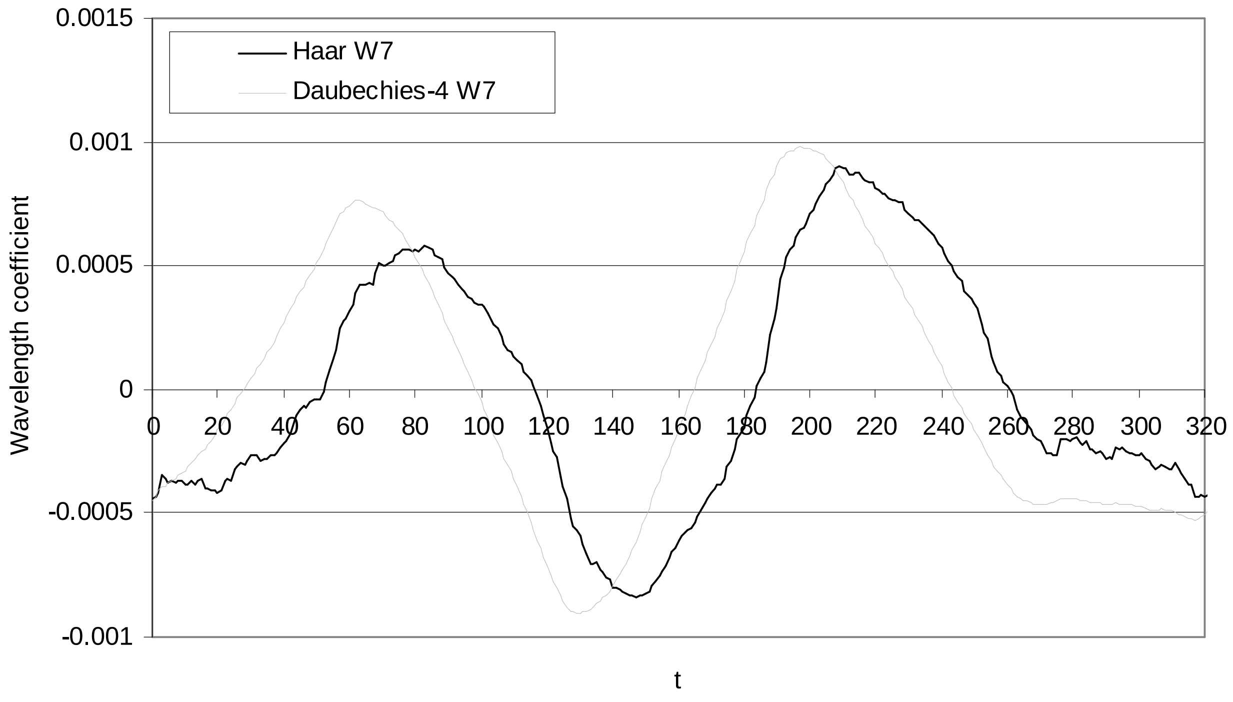

Figure 5 Wavelet coefficients $W_{j,t}$ as a function of t for j = 7. The maximum overlap $W_{j,t}$ is observed for t = 83 and t = 209 in case of the Haar wavelet analysis and for t = 63 and t = 199 in case of the Daubechies-4 wavelet analysis.

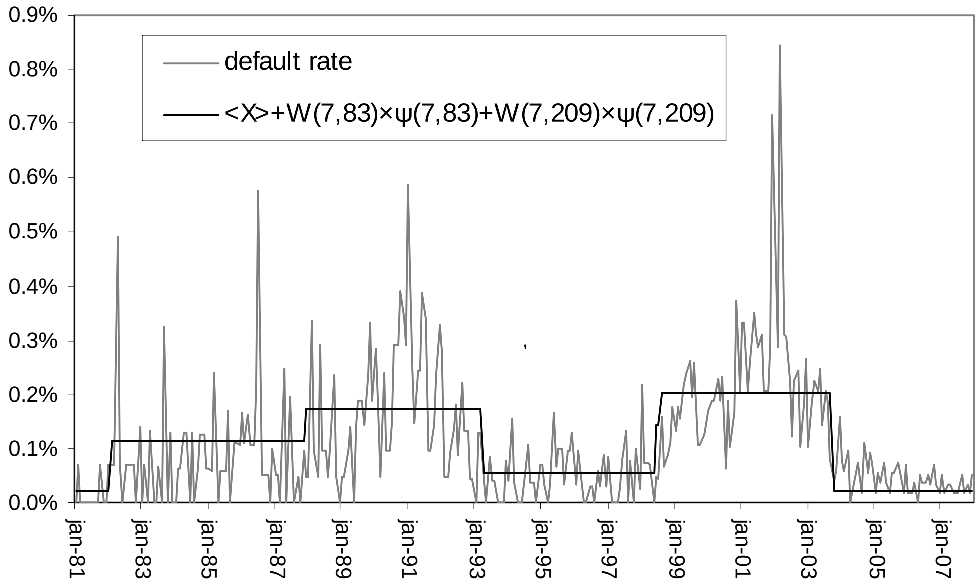

Figure 6 Montly default rates compared with the linear wavelet combination $<X>+W_{7,83}\psi^{H}_{7,83}+ W_{7,209}\psi^{H}_{7,209}$.

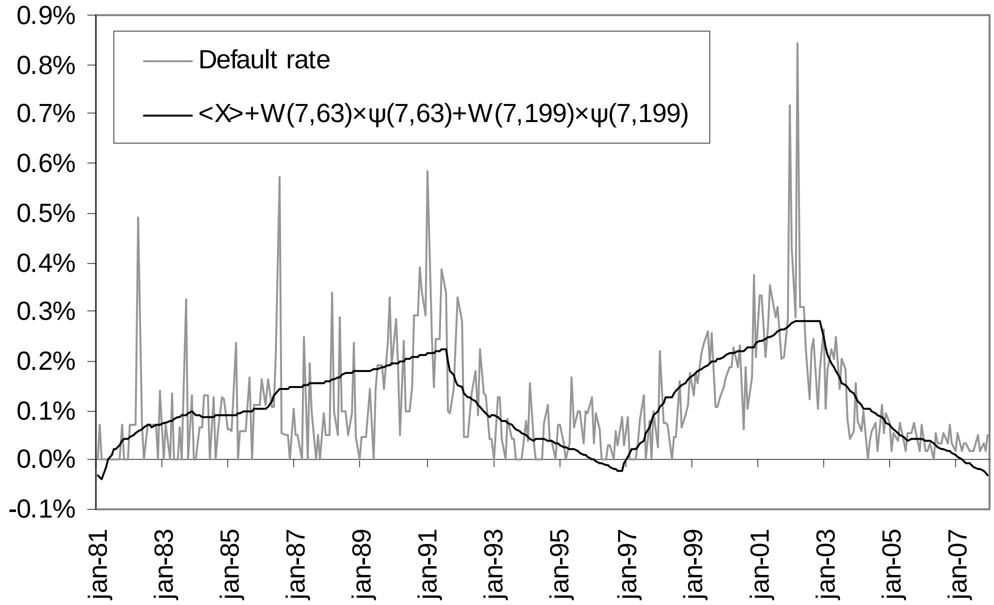

Figure 7 Montly default rates compared with the linear wavelet combination $<X>+W_{7,63}\psi^{D}_{7,63}+ W_{7,199}\psi^{D}_{7,199}$.

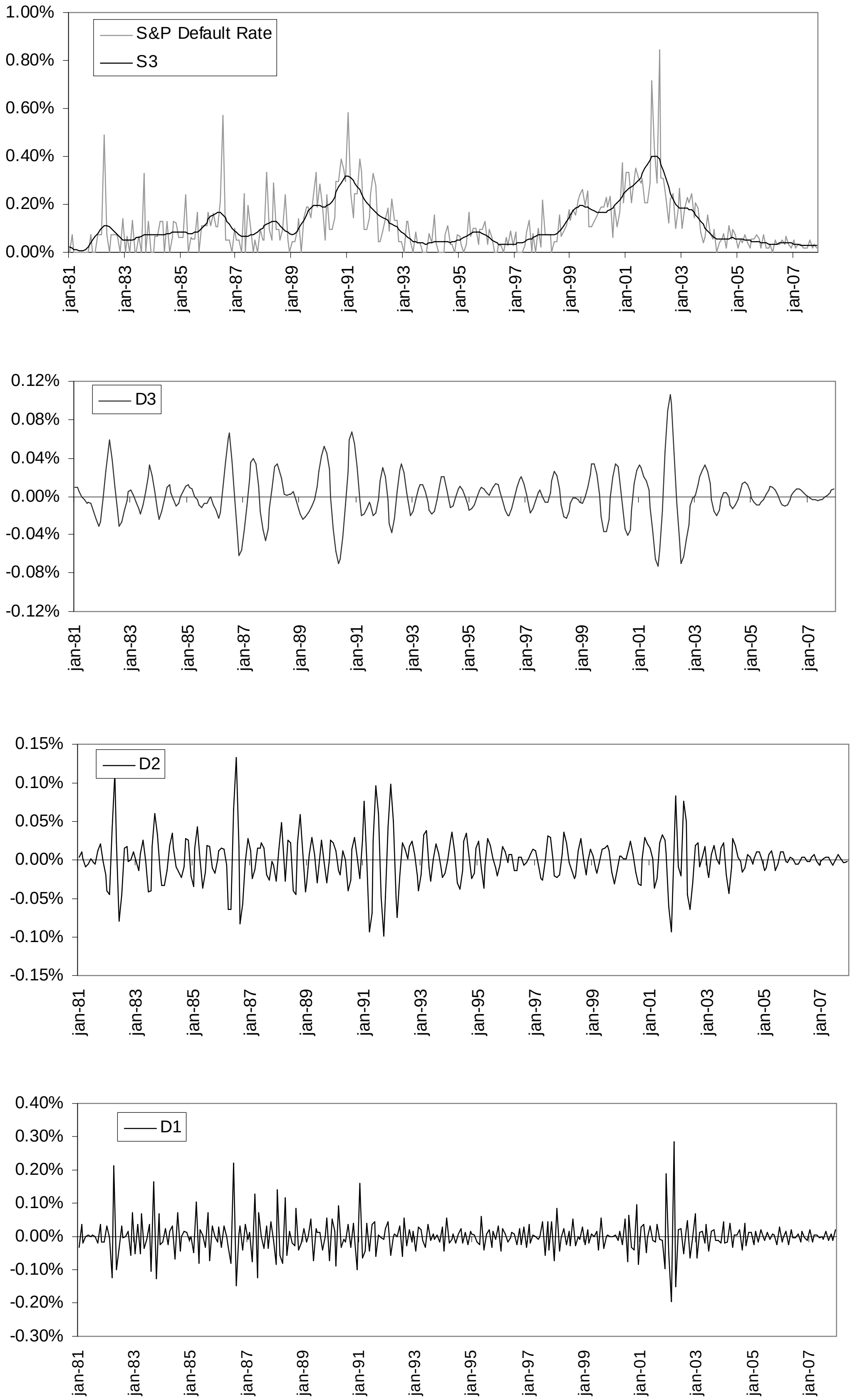

Figure 8 Multi-resolution analysis of the S&P monthly default rates (X). The time series X of default rates is decomposed up to level J = 3: X = S3 + D3 + D2 + D1. The highest graph shows the original and smoothed time series.

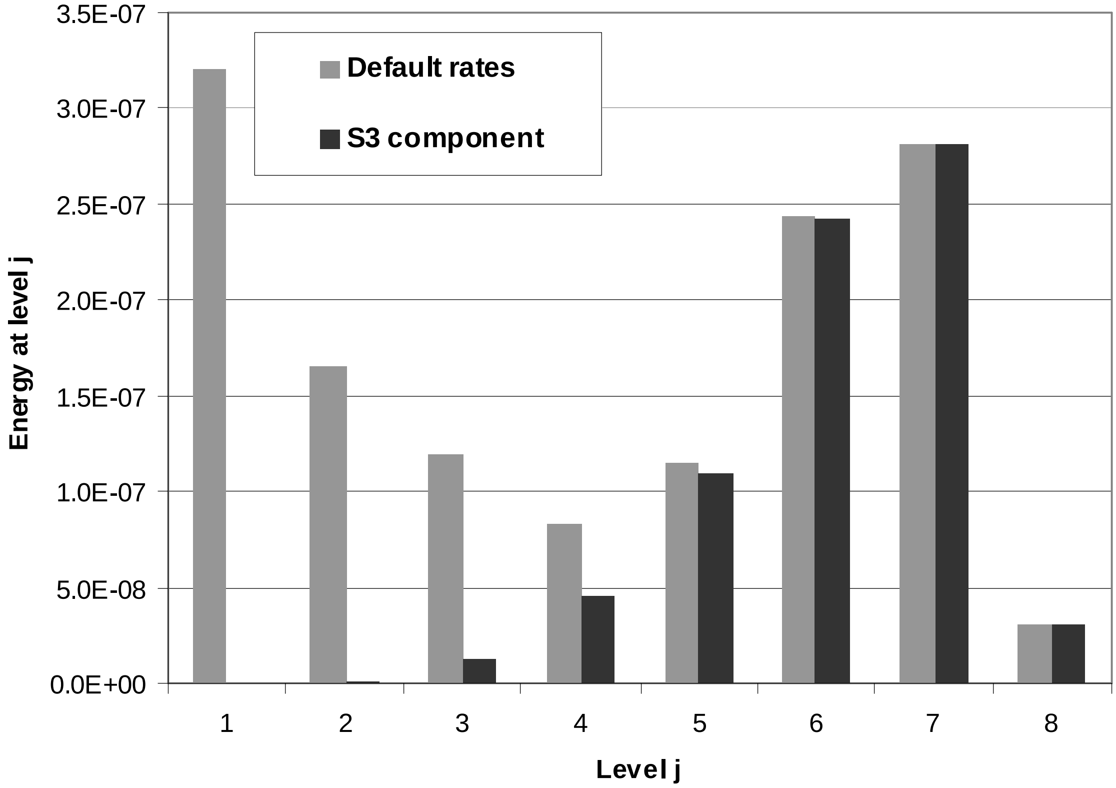

Figure 9 Energy spectrum of wavelet coefficients of monthly default rates and the smoothed S_3 component of the default rates. As a result of the smoothing, high frequencies are filtered out. The energy at level 7 contributes to 38.49% of the total variance.

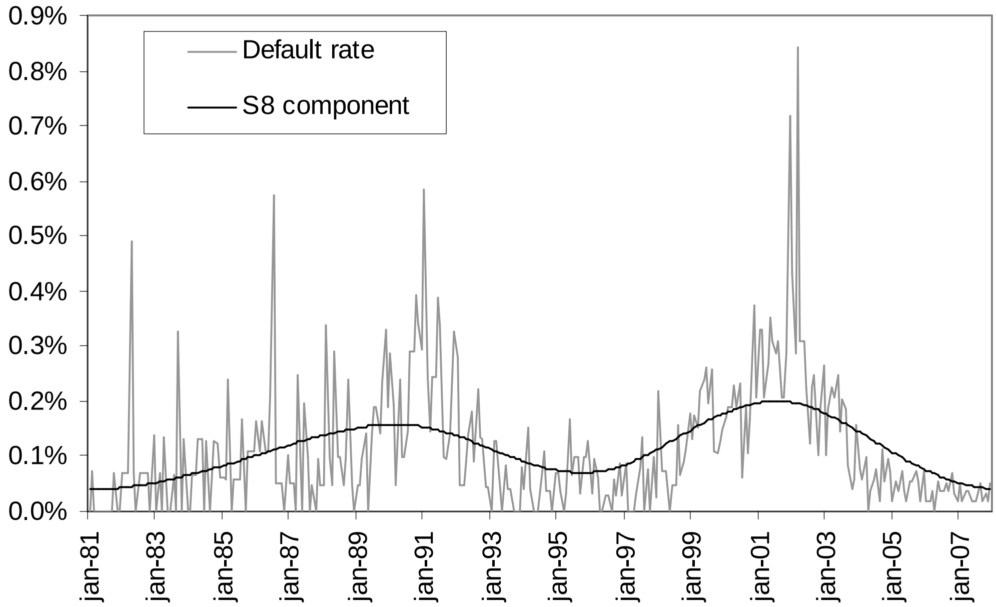

Figure 10 Time series of monthly default rates compared with its smoothed S_8 component. The S_8 component shows a slight upward tendency of 0.0017% per year.